

Sulfolane with LiPF₆, LiNTf₂ and LiBOB - as a non-Flammable Electrolyte Working in a lithium-ion batteries with a LiNiO₂ Cathode

Beata Kurc

Institute of Chemistry and Electrochemistry, Faculty of Chemical Technology, Poznan University of Technology, Berdychowo 4, PL-60965 Poznan, Poland

E-mail: beata.kurc@put.poznan.pl

Received: 1 March 2018 / Accepted: 11 April 2018 / Published: 10 May 2018

LiNiO₂ was examined as cathode materials for the lithium-ion battery, working with non-flammable electrolyte, obtained by dissolution of solid lithium bis(trifluoromethanesulphonyl)imide (LiNTf₂), lithium bis(oxalato)borate (LiBOB) and lithium hexafluorophosphate (LiPF₆, Fluka) in sulfolane (TMS) with 10% vinylene carbonate (VC). Apart from the electrochemical tests, it was important to set the flash point. The Li/LiNiO₂ cells were tested by cyclic voltammetry, galvanostatic charging/discharging. The LiNiO₂ cathode showed good cyclability and coulombic efficiency for the electrolyte, which contains 1 M LiPF₆ in TMS + 10% VC (195 and 140 mAh g⁻¹ after 20 cycles – C/10). Correspondingly lower capacity was observed for system Li/LiNiO₂ in: 1 M LiNTf₂ in TMS + 10% VC and 1 M LiBOB in TMS + 10% VC. The LiNiO₂(solid) + 1 M LiPF₆ + TMS + 10% VC system shows a flash point of ca. 160.

Keywords: sulfolane, li-ion battery, cathodes: LiNiO₂, impedance spectra

1. INTRODUCTION

Cathode material of lithium-ion battery should contain lithium or lithium ions, which can be intercalated/deintercalated during charging/discharging process. Cathode materials should: have ability of giving and taking as many as possible lithium ions in order to increase the capacity; both redox forms of cathode should be chemically stable; have good electronic conductivity to minimize the polarization of electrodes; reaction of electron exchange should occur at high potential vs. anode to maximize voltage of the cell; be environment friendly; be light to decrease the weight of the battery[1-4].

Cathode material of lithium-ion battery should contain lithium or lithium ions, which can be intercalated/deintercalated during charging/discharging process.

Nowadays the most popular cathode materials are LiCoO_2 and LiNiO_2 with 2D structure and LiMn_2O_4 with 3D structure. Due to the lower cost of obtaining and lower toxicity it would be more beneficial to use LiNiO_2 instead of LiCoO_2 . It turned out, however, that this material is difficult to obtain while maintaining the correct stoichiometric composition. Regardless of the experimental conditions, divalent nickel ions are always present, with half of them occupying lithium sites in the space between the layers [5]. It was also found that LiNiO_2 easily releases oxygen during operation at high potentials, thereby destroying its layered structure and leading to dangerous exothermic reactions with the organic electrolyte [6]. Despite the high capacity ($\sim 200 \text{ mAh g}^{-1}$) and low price, LiNiO_2 is not widely used in commercial cells. Li_xNiO_2 , like Li_xCoO_2 , form alternating layers of lithium and octahedrons NiO_6 with trigonal symmetry. The individual NiO_6 structures are connected with each other by common edges forming a grid of triangularly arranged Ni atoms. Material properties are strictly dependent on the stoichiometric composition. The general record is taken as: $\text{Li}_x\text{Ni}_{2-x}\text{O}_2$ ($0 < x < 1$). If the value of x decreases, the number of Ni^{2+} ions increases and thus the amount of active Li ions decreases, which ultimately affects the electrochemical capacity and the efficiency of the cell [7,8,9]. Difficulties in the synthesis of LiNiO_2 with the correct stoichiometric composition also result from the loss of lithium from the structure during high temperature calcination, caused by the high vapor pressure of lithium [9]. LiNiO_2 can undergo a reversible transformation from the hexagonal phase to the cubic [10]. If LiNiO_2 is sintered at a temperature above the phase transition temperature (around $720 \text{ }^\circ\text{C}$), it will contain a certain amount of inactive cubic form, eventually leading to a reduction in the electrochemical capacity of the material. Another problem is the loss of capacity also observed for the stoichiometric LiNiO_2 , as a result of the formation of NiO_2 during the irreversible phase transition occurring while charging the cell (Li^+ deproliferation) above 4 V vs. Li/Li^+ [11]. Although LiNiO_2 can occur in two structural variants, only the hexagonal structure is electrochemically active [12]. Therefore, the electrochemical capacity strongly depends on the structural parameters, which in turn depend on the synthesis conditions [13]. Despite the similarity of LiNiO_2 and LiCoO_2 , the mechanism of lithium ion insertion and de-copying in both materials takes place in a different way. Li-ions from LiNiO_2 can not be fully 'inserted' during the next reduction process due to structural changes. Therefore, the practical specific capacity of the material is from about 125 mAh g^{-1} to 150 mAh g^{-1} [14]. In the case of LiCoO_2 this problem does not occur due to the total reversibility during the first charge/discharge cycle [15]. To reduce the instability of LiNiO_2 , many studies on the modification of the material have been carried out, e.g. by substituting other cations for a portion of Ni^{3+} ions. It has been found that replacement of 20-30% Ni^{3+} with Co^{3+} ions gives adequate stability [16]. Among the modification techniques adopted, substitution of electrochemically neutral cations, i.e. Al, Mg, Ti or Mn as substitutes for Ni, proved to be effective. In addition, simultaneous subsidies with many metal ions proved to be an even better solution thanks to liquidation phase changes occurring during the cyclic cell operation [17,18]. Another approach was to modify the surface of the material with coatings of electrochemically inactive metal oxides [19,20,21]. Chowdari showed that coating $\text{LiNi}_{0.8}\text{Co}_{0.2}\text{O}_2$ with TiO_2 improves the cyclic performance of the material. He also stated that subsidizing with Ti ions or coating with TiO_2 layer are effective, introducing significant changes in the structure of LiNiO_2 and

LiCoO₂ cathodes [22]. However, it should be remembered that the processes of subsidizing and coating with metal oxides play different roles in improving the electrochemical efficiency of the cathode. The reduction of crystal lattice changes (phase transitions) is possible due to the introduction of other metals, while the improvement of interfacial stability due to oxide coatings [23].

The novelty and the essence of the research is to examine the work of a Li/LiNiO₂ cell with three non-flammable electrolyte: 1 M LiPF₆ in TMS + 10% VC; 1 M LiNTf₂ in TMS + 10% VC and 1 M LiBOB in TMS+ 10% VC.

2. EXPERIMENTAL

2.1. Materials

To prepared electrodes and electrolytes it was used: graphite, (G, SL-20, Superior Graphite, USA), poly(vinylidene fluoride) (PVdF, Fluka), sulfolane (TMS, Fluka), lithium foil (Aldrich, 0.75 mm thick), vinylene carbonate (VC, Aldrich), *N*-methyl-2-pyrrolidinone (NMP, Fluka), lithium bis(trifluoromethanesulfonyl)imide (LiNTf₂, Fluka), lithium hexafluorophosphate (LiPF₆, Fluka), lithium bis(oxalato)borate (LiBOB Fluka), LiNiO₂ powder (Aldrich) were used as purchased.

Electrolytes were obtained by dissolution of the solid LiPF₆, LiNTf₂ and LiBOB salts in liquid TMS heated to ca. 35 °C (TMS is solid at room temperature). Electrolytes contained VC as a SEI forming additive (10%). Tested LiNiO₂ cathode were prepared by casting LiNiO₂ + G + PVdF (ratio 85:5:10) slurry in *N*-methyl-2-pyrrolidinone (NMP, Fluka) on the current collector (diameter 12 mm) (NMP was evaporated in vacuum at 120 °C).

2.2. Apparatus and measurements

Particle size distributions was determined for LiNiO₂. Measurements were performed on a Zetasizer Nano ZS made by Malvern Instruments Ltd. UK, using the non-invasive back scattering method (NIBS). From the particle size distribution the polydispersity index was calculated, which provides information on the homogeneity of the product particles. The morphology and microstructure of the products were examined using a scanning electron microscope (Zeiss EVO40). From these images it was also possible to determine the particle structures and their tendency towards aggregation or agglomeration.

The electrochemical properties were characterized using galvanostatic charge-discharge tests (Atlas-Sollich, Poland), cyclic voltammetry (CV) and ac impedance measurements (μ Autolab FRA2 type III electrochemical system - Ecochemie, Netherlands). Cycling efficiency of LiNiO₂ | Li system was measured in two compartment cells. Electrodes were separated by the glass microfiber GF/A separator (Whatmann), placed in an adopted 0.5 Swagelok® connecting tube. The mass of electrodes was as follows: Li: ca. 45 mg (0.785 cm²) and cathode: 2.0–3.0 mg. The cells were assembled in a glove box in the dry argon atmosphere and the cycling measurements were taken at different current rates (C/10–C/2).

Moreover thermal gravimetric analysis was conducted (STA 449 F3 Jupiter TG/DTA analyser - NETZSCH-Gerätebau GmbH) with the $2\text{ }^{\circ}\text{C min}^{-1}$ rate. Flash point of the electrolyte was measured with an open cup home-made apparatus (it was reported in[24]).

3. RESULTS AND DISCUSSION

3.1. PSD and morphology

Figure 1 shows particle size distributions and SEM images of LiNiO_2 (a, b) respectively. LiNiO_2 is characterised by a monomodal particle size distribution with diameters in the range 825-1720 nm (Fig. 1a). As evidenced by the SEM image (Fig. 1b) the particles are regular in shape. The cathode is highly homogeneous, as is confirmed by the low polydispersity index of 0.326.

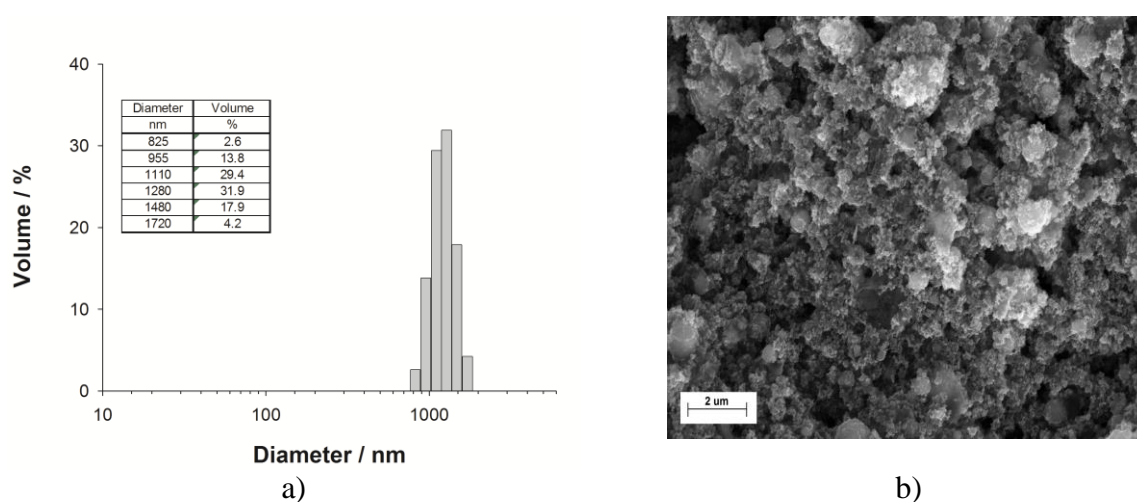


Figure 1. PSD of LiNiO_2 a) and SEM image of LiNiO_2 b)

3.2. Electrolyte liquidity range, viscosity and conductivity

Sulfolane is an important technical solvent in many extraction processes. It also has an ability to extract selectively aromatic hydrocarbons from aliphatic ones and to absorb waste gases which makes it very useful in the petrochemical industry. There are many applications of sulfolane in photographic emulsions, fabrics manufacturing, wood chips impregnation and polymer plasticizing [25]. One of the most important parameters taken into account in the case of solvents used as electrolytes in electrochemical devices is viscosity. For example, ionic liquids are highly viscous due to the strong coulombic (electrostatic) interaction between ions. Strong interactions between ions also translate into ion mobility.

Silne oddziaływania pomiędzy jonami przekładają się również na ruchliwość jonów.

The sulfur-oxygen double bond is highly polar, ensuring the miscibility of sulfolane with water, while the carbon backbone affects good solubility in hydrocarbons, whereby sulfolane is widely used as a solvent for the purification of hydrocarbon mixtures.

The physicochemical properties of sulfolane have been described in detail in previously works - melting point (301.6 K (ca. 28 °C)) [24]); boiling point and cryoscopic constant; conductivity of the electrolyte (at $T = 298$ K is 2.6 mS cm^{-1}), with the activation energy of the conduction process, ($E_{\sigma}^a = 18.4 \text{ kJ mol}^{-1}$ [25]); viscosity, η , (ca. 10 cP at 30 °C) [24].

3.3. Charging/discharging

Literature sources contain much information on the obtained capacity for the discussed cathode [26-35] (Table 1).

Table 1. Capacity of the LiNiO_2 cathode materials.

MATERIAL	CAPACITY	REFERENCES
Reacting LiNO_3 with Ni(OH)_2 or NiCO_3 at 750 °C under an O_2 atmosphere produced a product	charge capacity of 180 mAh g^{-1} and a reversible discharge capacity: 150 mAh g^{-1} (voltage range of 2.5–4.2 V)	28
LiNiO_2 at a high O_2 flow rate (800 mL min^{-1}),	4160 mAh g^{-1} with 150 mAh g^{-1} remained after 30 cycles (3.0–4.3 V, 0.4 mA cm^{-2})	29
LiNiO_2 obtained by mixing an aqueous solution of $\text{LiOH/H}_2\text{O}$ and $\text{Ni(NO}_3)_2/6\text{H}_2\text{O}$ (molar ratio of 4:1); washing away the large amount of excess Li after calcination.	reversible capacity: 200 mAh g^{-1} during 10 cycles (3.0–4.5 V, 0.5 mA cm^{-2})	30
The synthesis of LiNiO_2 using the precipitated nickel hydroxide precursor followed the protocol originally designed for lithium nickel-manganese-cobalt oxide	capacity of 223 mAh g^{-1} in the first charge, and 190 mAh g^{-1} in the first discharge	31
$\text{LiNi}_{0.8}\text{Co}_{0.1}\text{Mn}_{0.1}\text{O}_2$ due to the formation of $\text{Li}_2\text{CO}_3/\text{LiOH}$ impurities and a spontaneous reduction of Ni^{3+} to Ni^{2+} on the surface	discharge capacity (148 mAh g^{-1} at 8C) and better capacity retention at 2 C (79.2% after 100 cycles)	32
The residual lithium compounds on the surface of Ni-rich layered $\text{LiNi}_x\text{Co}_y\text{Mn}_{1-x-y}\text{O}_2$ materials - $\text{LiNi}_{0.8}\text{Co}_{0.1}\text{Mn}_{0.1}\text{O}_2$ material	discharge capacity of $160.65 \text{ mAh g}^{-1}$ (capacity retention of 86.95% after 100 cycles at 55 °C and the current rate: 2C). Pristine material ($131.57 \text{ mAh g}^{-1}$ and 74.90%).	33
LiNiO_2 with Ni defects in the 3b sites	The reversible capacity was 212 mAh g^{-1} discharge capacity of 214 mAh g^{-1} in a	34
$\text{LiNi}_{0.9}\text{Co}_{0.1-x}\text{Ti}_x\text{O}_2$ ($0.02 \leq x \leq 0.05$) cathode materials	charge/discharge capacity: 200 mAh g^{-1} (voltage range of 3.0–4.3 V (vs. Li/Li^+)), capacity retention of 98.7% (after 50th cycles)	35

An intercalation cathode is a solid host network, which can store guest ions. The guest ions can be inserted into and be removed from the host network reversibly. In a Li-ion battery, Li^+ is the guest ion and the host network compounds are metal chalcogenides, transition metal oxides, and polyanion compounds. These intercalation compounds can be divided into several crystal structures, such as layered, spinel, olivine. The layered structure is the earliest form of intercalation compounds for the cathode materials in Li-ion batteries. LiNiO_2 (LNO) has same crystal structure with LiCoO_2 and a similar theoretical specific capacity of 275 mAh g^{-1} . Its relatively high energy density and lower cost compared to Co based materials are the main research driving forces. However, pure LNO cathodes are not favorable because the Ni^{2+} ions have a tendency to substitute Li^+ sites during synthesis and delithiation, blocking the Li diffusion pathways [16]. Partial substitution of Ni with Co was found to be an effective way to reduce cationic disorder [18].

The half-cells was tested for 50 cycles, but figures 2-4 present charging/discharging for the first 20 cycles.

Figures 2-4 show charge-discharge curves and coulombic efficiency of the Li/ LiNiO_2 half cell using: 1 M LiPF_6 in TMS + 10% VC (Fig. 2); 1 M LiNTf_2 in TMS + 10% VC (Fig. 3) and 1 M LiBOB in TMS+ 10% VC (Fig. 4).

The highest capacity is observed for the system $\text{Li} \mid 1 \text{ M LiPF}_6 \text{ in TMS} + 10\% \text{ VC} \mid \text{LiNiO}_2$. The capacity of the charging (deintercalation) and discharging (intercalation) processes after 20 cycles was 200 mAh g^{-1} and 195 mAh g^{-1} , resulting in a coulombic efficiency of 98% under the current rate C/10. Moreover when the current is increased from C/10 to C/2 charge and discharge capacity decreases after 20 cycles to 144 mAh g^{-1} and 135 mAh g^{-1} , respectively (Fig. 2). The reversible capacity is not low and accounts for 70% of the theoretical value, which is a good result with promising prospects for further research.

The genital operation of the cathode with tested electrolytes gives a stable system capacity. Differences are noticeable in the reversibility of the cell. The electrolyte containing LiPF_6 in TMS provides comparable results with the data included in table 1. The capacity obtained at level 200 is very good for the cathode material being tested.

Slightly worse properties of the LiNiO_2 cathode are observed for other electrolytes. The charging/discharging capacity for $\text{Li} \mid 1 \text{ M LiNTf}_2 \text{ in TMS} + 10\% \text{ VC} \mid \text{LiNiO}_2$ is found within a range of $180\text{-}170 \text{ mAh g}^{-1}$ and $170\text{-}162 \text{ mAh g}^{-1}$ resulting in a coulombic efficiency of 95% (current is increased than charge and discharge capacity decreased) (Fig. 3).

The lowest coulombic efficiency, of about 90%, is observed for the system $\text{Li} \mid 1 \text{ M LiBOB in TMS} + 10\% \text{ VC} \mid \text{LiNiO}_2$. The electrolyte containing LiBOB was the least stable during the charging/discharging process (Fig. 4).

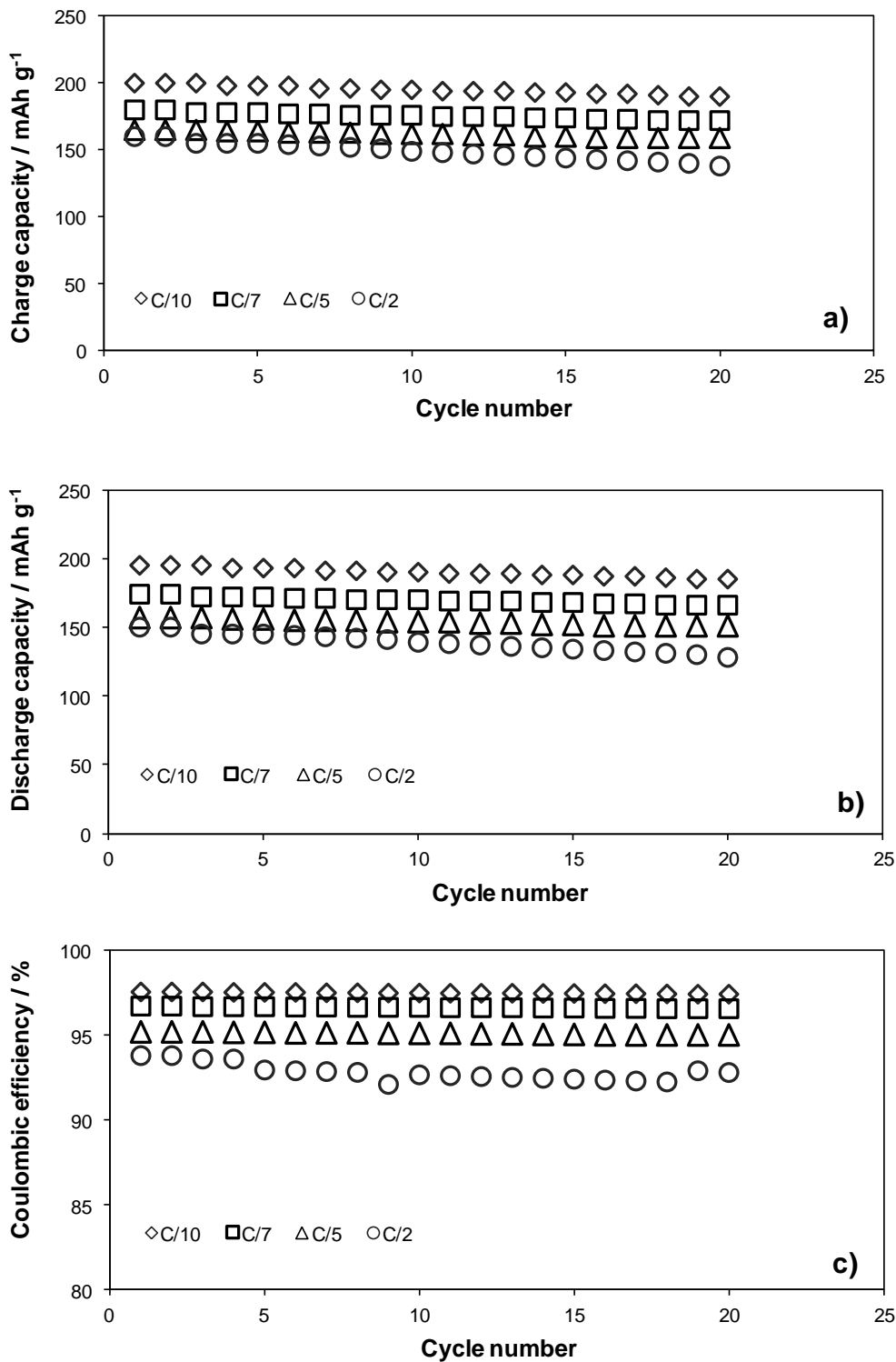


Figure 2. Charging capacity a) Discharging capacity b) Coulombic efficiency c) of the cell: LiNiO₂|1 M LiPF₆ in TMS + 10% VC |Li (rates: C/10, C/7, C/5, C/2).

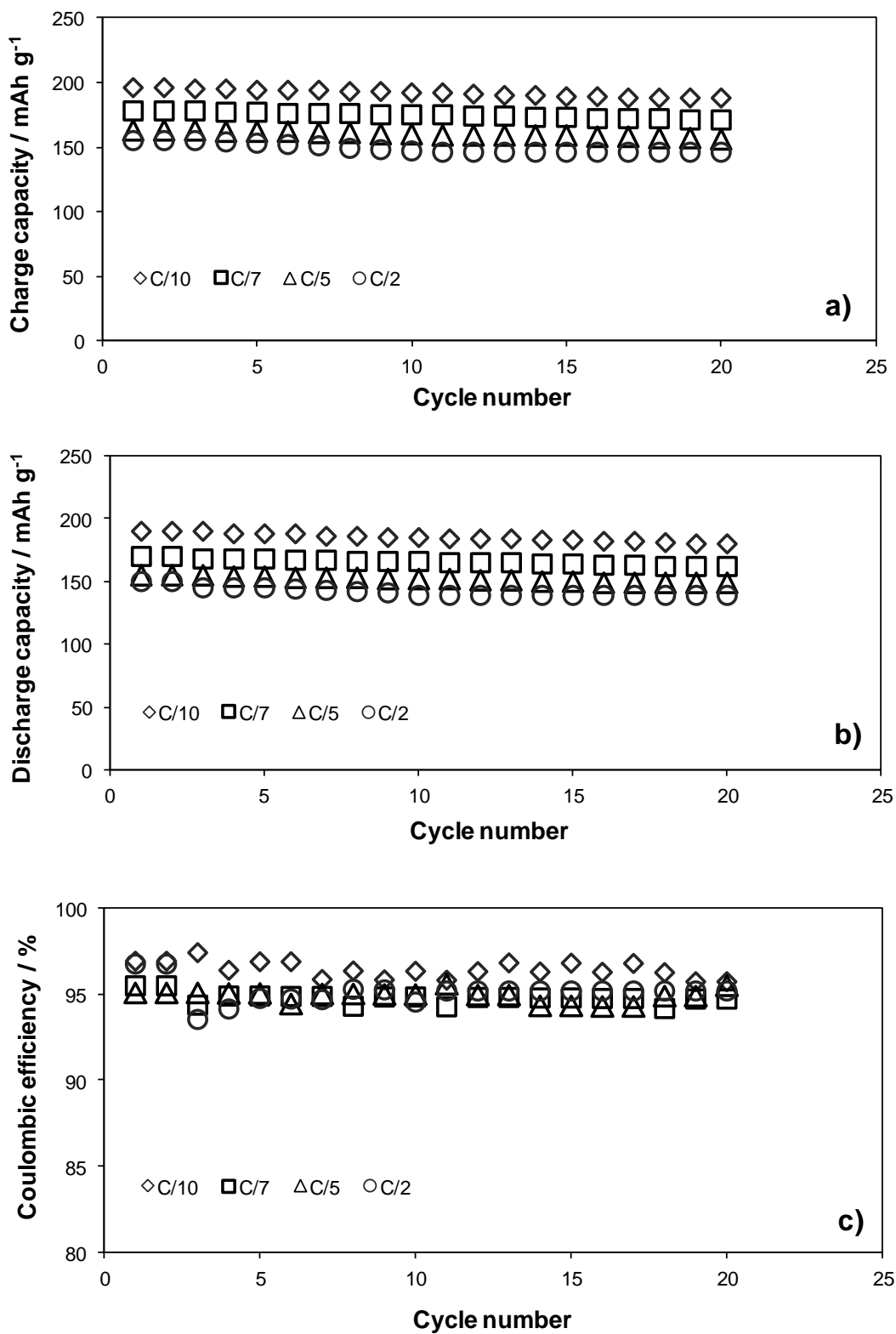


Figure 3. Charging capacity a) Discharging capacity b) Coulombic efficiency c) of the cell: LiNiO₂|1 M LiNTf₂ in TMS + 10% VC |Li (rates: C/10, C/7, C/5, C/2).

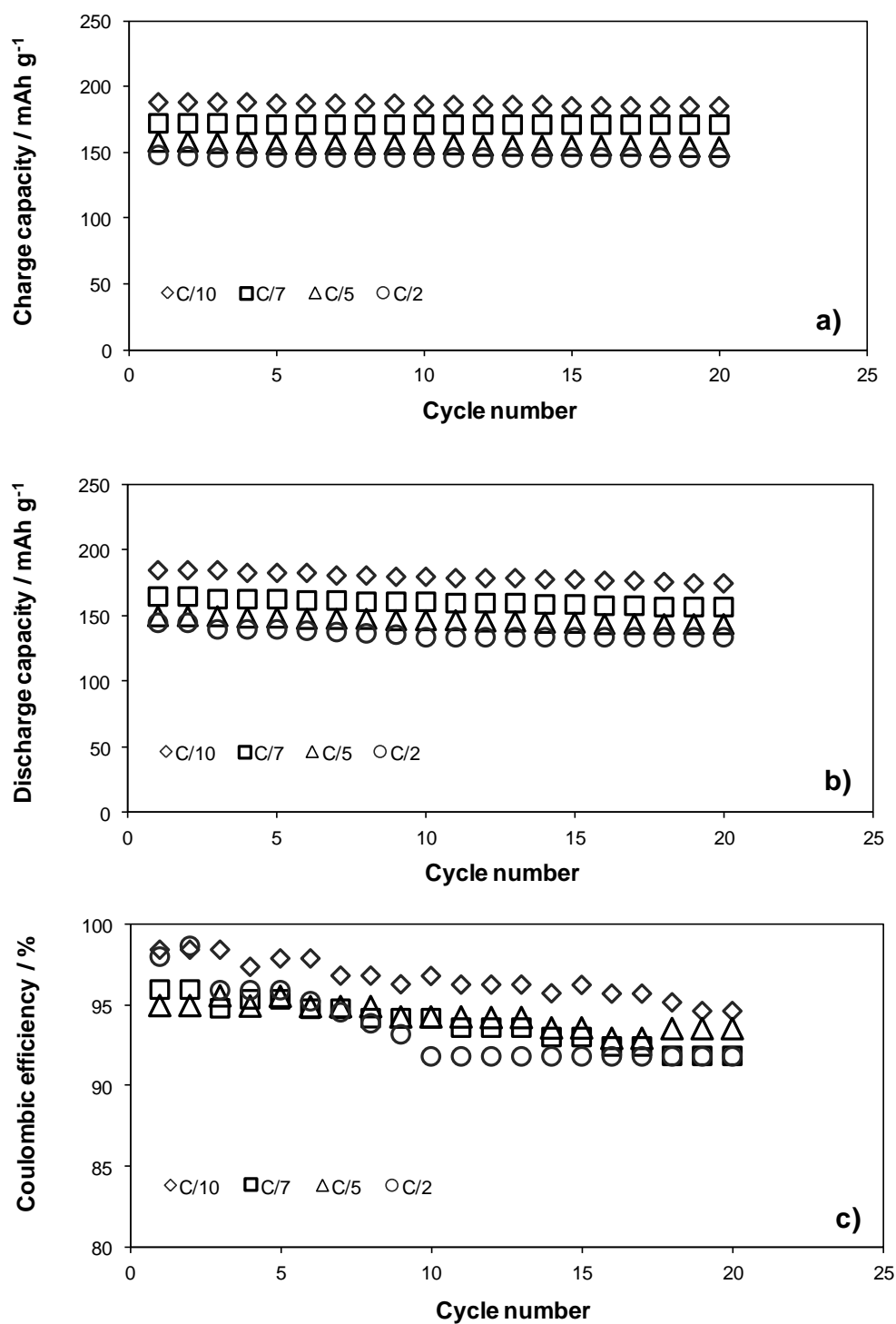


Figure 4. Charging capacity a) Discharging capacity b) Coulombic efficiency c) of the cell: LiNiO₂|1 M LiBOB in TMS + 10% VC |Li (rates: C/10, C/7, C/5, C/2).

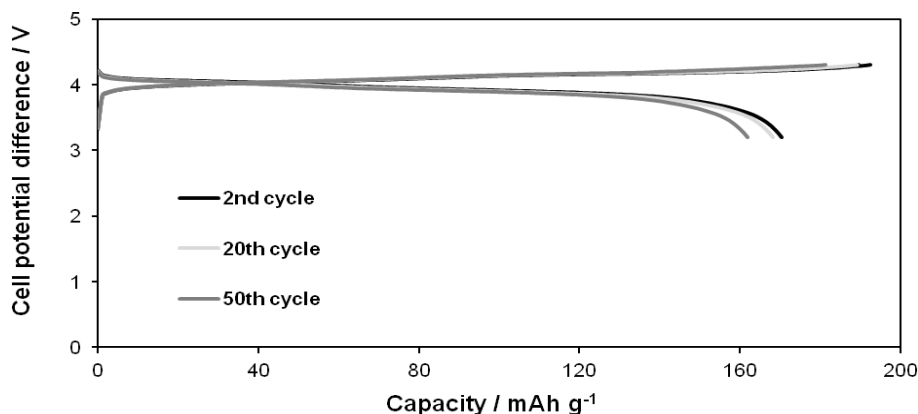


Figure 5. Galvanostatic charging and discharging of: a) $\text{LiNiO}_2/1 \text{ M LiPF}_6$ in TMS + 10 % wt. VC/Li, (2^{nd} , 20^{th} , 50^{th} cycles) at C/5 rate.

3.4. Electrolyte flammability

Sulfolane (tetrahydrothiophene 1,1- dioxide or tetramethylene sulfone) is rarely used as non-aqueous solvents. Sulfolane has many advantages such as chemical and thermal stability, high polarity, low autoprotolysis constant, low vapor pressure and relatively low toxicity. There are of course few drawbacks of sulfolane such as relatively high viscosity, hygroscopicity and high melting point. The melting point is compensated for by a very high cryoscopic constant ($\sim 65 \text{ deg kg mol}^{-1}$). The cost of sulfolane is also high in comparison to other more common dipolar aprotic solvents.

Table 2. Flash point of the substances

PRODUCTS	FLASH POINT / °C
Ethylene carbonate (EC)	143
Propylene carbonate (PC)	123
Dimethyl carbonate (DMC)	16
Sulfolane (TMS)	176
LiNiO_2 (solid) + 1 M LiPF_6 + TMS + 10% VC	160
LiNiO_2 (solid) + 1 M LiPF_6 + EC 50% + DMC 50%	44
LiPF_6 solution in TMS, without VC	170
LiNTf_2 solution in TMS, without VC	158
LiPF_6 solution in TMS, without VC	155

Flash points of the substances are shown in Table 2. During SEI formation the volatile additive (VC) is converted into a solid polymeric component of the interface. Consequently, the amount of the volatile compound decreases to a low value, increasing the flash point of the electrolyte.

Pure sulfolane is an odorless and colorless solid with melting point at 28°C (TMS is solid at room temperature [24]). 1.3% water by weight reduces the freezing point to 17.2°C . To avoid water traces in sulfolane due to its high hygroscopicity, the purified products should be stored under dry nitrogen. Sulfolane because of its great hygroscopicity is miscible in water in all proportions. Many organic compounds are also soluble in sulfolane. As far as the alkali metal chlorides are concerned, the

best solubility in sulfolane exhibit LiCl (361 mmoles/liter). The commercial manufacture of sulfolane is based on the Diels-Alder reaction of butadiene and sulfur dioxide. This reaction depends on the temperature and concentration of the reactants. There are also several alternative methods based on oxidation of tetrahydrothiophene. In these methods several different oxidants in the presence or absence of catalyst have been used in different reaction media. There are also few drawbacks of sulfolane such as wettability, poor cathodic stability on carbonaceous anodes. Wettability problems were identified when using sulfone based electrolytes. Need ceramic or ceramic coated separators for maximum performance.

Due to the very low volatility, for example, of ionic liquids, determining the boiling points of these compounds often becomes problematic due to their thermolysis before reaching the boiling point. Therefore, you can determine their thermal stability for additional information. In most cases, thermogravimetric analysis (TGA, thermogravimetry - TG) is performed, which provides information on the temperature of decomposition of the tested compounds. The differential scanning calorimetry (DSC) can also be used to measure the heat of phase transformations.

Figure 6 shows thermal gravimetric analysis (TG/DTA) of the 1 M LiPF₆ + TMS + 10% VC electrolyte under nitrogen atmosphere. It can be seen that the main decomposition peak of the electrolyte (both liquid solvents and the lithium salt) is found at ca. 275 °C. The TG/DTA profiles shown in Fig. 6 are similar to those found for a polyvinylidene fluoride-based gel electrolyte [42].

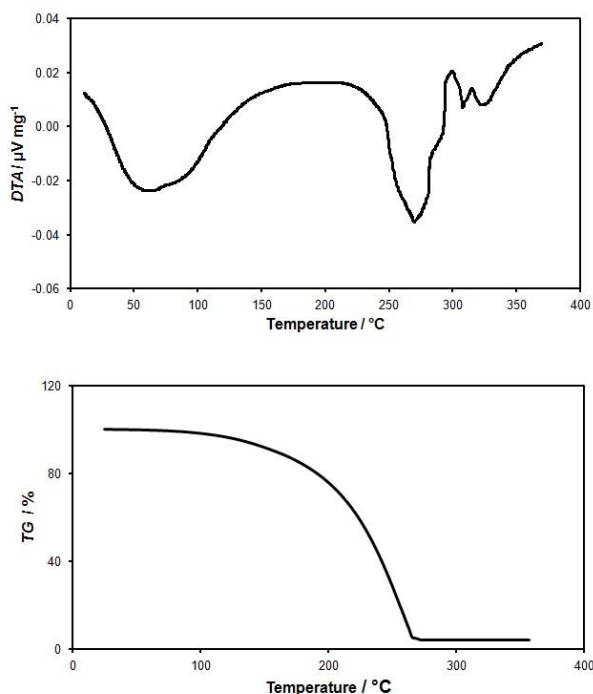


Figure 6. TG/DTA profiles related to the heating test of the 1 M LiPF₆ + TMS + 10% VC electrolyte under nitrogen atmosphere.

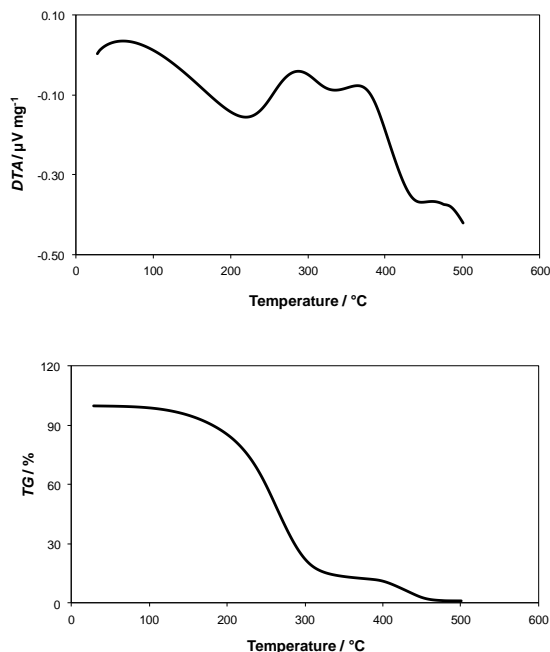


Figure 7. TG/DTA profiles related to the heating test of the 1 M LiNTf₂ + TMS + 10% VC electrolyte under nitrogen atmosphere.

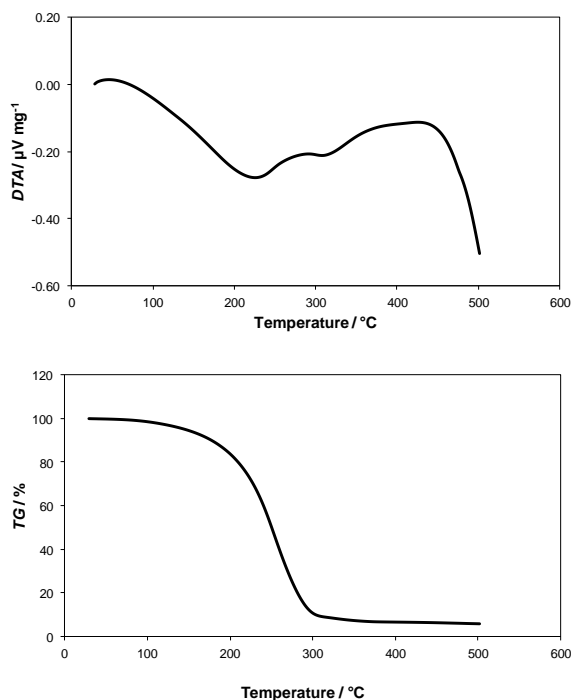


Figure 8. TG/DTA profiles related to the heating test of the 1 M LiBOB + TMS + 10% VC electrolyte under nitrogen atmosphere.

No significant differences were observed in the TG/DTA for other electrolytes (1 M LiNTf₂ + TMS + 10% VC or 1M LiBOB + TMS + 10% VC). The peak appears at approximately 260-280 $^{\circ}\text{C}$ (Figs. 7 and 8).

The current lithium ion battery has a problem with safety connected with the use of readily volatile and highly flammable organic carbonates as electrolytes. Recent efforts have been focused on finding electrolyte that are non-flammable and has a high flash point. There are reported use of sulfone compounds as electrolyte additives in ILs, such as ionic liquid/sulfone mixed electrolyte based on N-butyl-methyl piperidinium bis(trifluoromethyl)sulfonyl imide (PP14-TFSI) and tetramethylene sulfone (TMS). Flammability test were held on TMS. The TMS ignited within 10s and continued burning after the flame was removed, because TMS is flammable at ambient temperature [36-38]. Advantages of sulfones as high voltage electrolyte: broad electrochemical stability windows – 5.0V; sulfones are known to be extraordinary anodic stable up to 5.5V vs. Li/Li⁺ [5]; high dielectric constants [24]; wide liquid phase temperature range [24]; low cost- byproduct in petroleum industry; excellent cycling performance for cells using EMS or TMS as electrolyte solvents. No capacity fade for 100 cycles.

3.5. Cyclic voltammetry

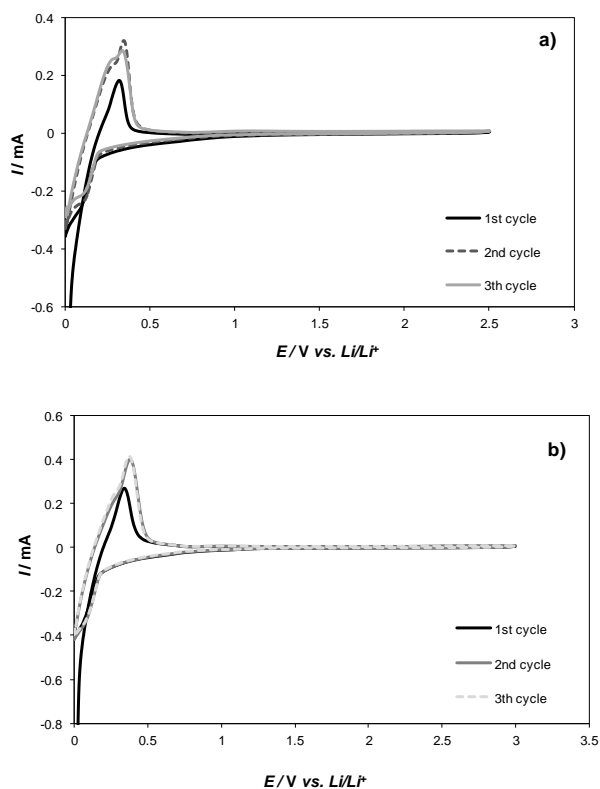


Figure 9. Cyclic voltammogram of graphite with: a) 1 M LiNTf₂ in TMS + 10% VC and b) 1 M LiBOB in TMS + 10% VC vs. Li/Li⁺. Scan rate: 0.1 mV s⁻¹

Sulfolates are suitable for operation as electrolytes of lithium-ion cells should have a wide range of electrochemical stability (low cathodic potential and high anode vs. Li / Li + potential), which

will enable the course of reversible redox reactions occurring both on the cathode and the anode during cell work.

A cyclic voltammogram of the Pt | 1 M LiPF₆ in TMS + 10% VC system is given in literature [68]. Cyclic voltammograms of the graphite electrode in 1 M LiNTf₂ dissolved in TMS is shown in Fig. 9a. Examination of the curve of the first cycle (the first reduction process) shows two fine peaks around 0.2 and 0.7 V, presumably corresponding to the formation of SEI on the surface anode.

These peaks which disappear completely with further cycling are apparently due to VC reductions. The next stage of lithium intercalation occurs at potential below 0.3 V and reaches a peak at a potential 0.005 V. The difference between the *cv* curve of the first cycle and subsequent cycles indicates that the irreversible capacity mainly occurs in the first cycle. A similar picture is observed in the case of the second electrolyte, i.e.: 1 M LiBOB dissolved in TMS (Fig. 9b).

3.6. Impedance studies

Lithium-ion batteries store electricity in electrodes composed of materials having the ability to reversibly intercalate (insert) lithium ions. During loading and unloading, Li⁺ ions are transferred via the electrolyte between two electrodes while oxidation and reduction processes occur. The electrolyte may be a liquid, a gel or a solid polymer, however, most cells use a liquid electrolyte consisting of a lithium salt (eg LiPF₆, LiBF₄, LiClO₄) dissolved in a mixture of organic solvents (liquid carbonates) such as ethylene carbonate (EC), dimethyl carbonate (DMC), diethyl carbonate (DEC) and methyl ethyl carbonate (EMC). In some cases, additives that stabilize the electrolyte interface/electrode, eg vinyl carbonate (VC), are also used. The lithium-ion cells operate at a voltage of the order of 4 V, giving the specific energy between 100 Wh kg⁻¹ and 150 Wh kg⁻¹. The classic link is built from a graphite anode, a cathode made of a lithium metal oxide (LiMO₂, e.g. LiNiO₂) and electrolyte. To avoid direct contact of the electrodes, they are separated by a separator, selectively permeable to lithium ions and well wettability by electrolyte. The most commonly used electrolyte is LiPF₆ salt solution in EC-DMC.

Lithium salts for LIB should be soluble in dipolar aprotic solvents at a concentration close to 1M. Such lithium salts should usually have a large anion to ensure a good dissociation in the solvents and limit the formation of ion pairs. In addition, these salts should be safe, environmentally friendly and must exhibit a high oxidation potential. In the literature, the most studied salts are lithium: perchlorate (LiClO₄), lithium hexafluorophosphate (LiAsF₆), lithium tetrafluoroborate (LiBF₄), lithium bis(trifluoromethanesulfonyl)imide (LiTFSI), lithium triflate (LiTf) and lithium hexafluorophosphate (LiPF₆), the most commercialized salt [37]. LiPF₆ is now a standard electrolyte for Li-ion cells, but this salt causes many problems [37]. Indeed, the success of LiPF₆ is mainly due to a combination of well-balanced properties such as ion mobility, ion pair dissociation, solubility, chemical inertness, surface chemistry (SEI) and collector passivation [24]. In solid state this salt decomposes at around 30 °C, and in solutions at around 80-85 °C (or lower), which can be problematic when the cell is discharged at high rates or stored at high temperatures [38]. The most thermally stable

salts are imide, triflate and perchlorate. The methide salt was shown to be thermally stable at around 350 °C.

Sulfones such as ethylmethylsulfone (EMS), methoxy-methylsulfone (MEMS) or tetramethylsulfone (TMS) are good candidates for the high voltage electrolytes (electric vehicles) as their electrochemical stability in the presence of LiPF_6 remains good up to 5 V vs. Li/Li^+ at the platinum electrode.

To confirm the validity of the performed tests, two-temperature tests were carried out. Elevated was to confirm the operation of the system as non-flammable and thermal resistance with potential application.

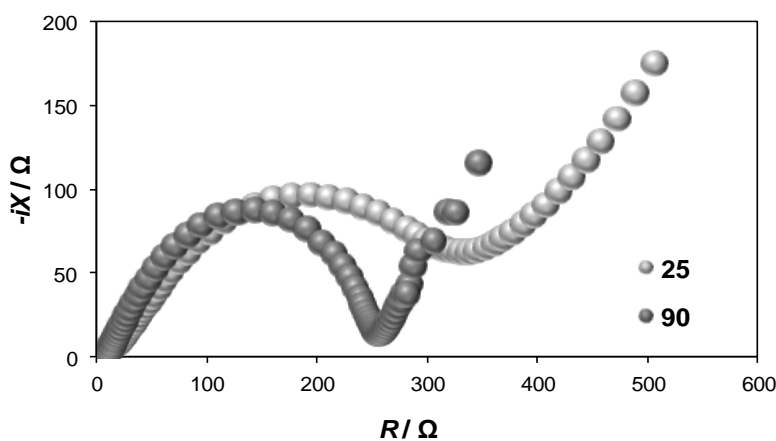
For a system containing a lithium salt: LiNTf_2 in TMS was decided to perform a comparative studies by performing temperature impedance spectrum.

Figure 10a presents impedance spectra of and $\text{LiNiO}_2|\text{LiNTf}_2$ in TMS|Li cell. Spectra were deconvoluted according to the equivalent circuit shown in Figure 10b. The conductivity of 1.0 M LiNTf_2 in TMS at 25 °C was 2.6 mS cm^{-1} , with the activation energy $E_\sigma^a = 18.4 \text{ kJ mol}^{-1}$. Therefore, the specific conductivity of the electrolyte at 90 °C was 9.6 mS cm^{-1} , which is comparable to the corresponding value characteristic of classical solutions in cyclic carbonates working at room temperature.

Corresponding resistance of the electrolyte in cells, R_{el} , was somewhat higher than that expected from its conductance, due to the porous structure of both electrodes. However, at 90 °C it decreased considerably to ca. $8 \text{ } \Omega$.

The resistance of the SEI layer, R_{SEI} , formed at 25 °C on the the LiNiO_2 cathode was ca. $51 \text{ } \Omega$, respectively. The corresponding value for SEI formed at 90 °C, was higher, achieving $67 \text{ } \Omega$ (LiNiO_2). A possible explanation is that at a higher temperature the thickness of the formed SEI layer was higher.

In this model, R_{el} , R_s and R_{ct} are the resistance of liquid electrolyte, the resistance of SEI film and the charge transfer resistance, respectively. The variations of R_{el} , R_s and R_{ct} are extremely important kinetic parameters which have a tight relationship with inside structural transformation and cycling stability [36].



a)

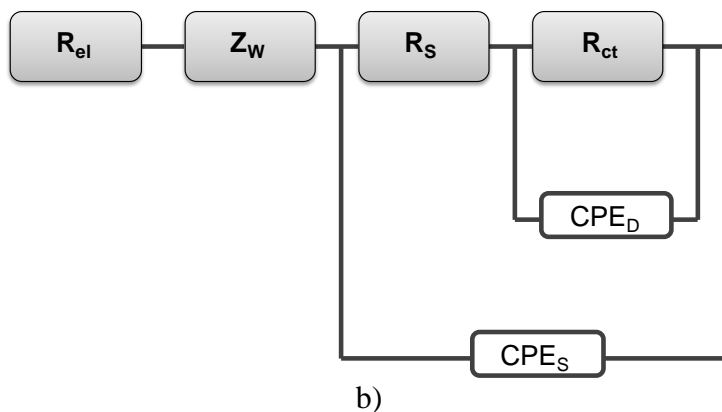


Figure 10. Impedance spectra of the $\text{LiNiO}_2|\text{Li}$ system as a function of temperature. LiNiO_2 mass: 2.80 mg (a) - electrodes were after three working cycles (intercalation deintercalation/intercalation). Equivalent circuit used for impedance spectra deconvolution of the $\text{LiNiO}_2|\text{SEI}|\text{Li}^+$

The corresponding charge transfer resistance for the $\text{LiNiO}_2|\text{Li}^+$ cathode (ca. 2.80 mg, BET specific area $15.4 \text{ m}^2 \text{ g}^{-1}$, real surface area $A = 431 \text{ cm}^2$) was lower: ca. $5.96 \times 10^{-5} \text{ A cm}^{-2}$ and $7.26 \times 10^{-5} \text{ A cm}^{-2}$ at $25 \text{ }^\circ\text{C}$ and $90 \text{ }^\circ\text{C}$, respectively.

The line at the low-frequency region is due to the diffusion of the electro-active species. Generally, any software system used for EIS curve deconvolution applies the Warburg model, which is based on a symmetrical constant phase element. Hence, the diffusion process was approximated here also by the Warburg element Z_w . Slopes of linear parts of impedance spectra were not exactly 45° , as predicted by the Warburg model. However, the LiNiO_2 cathode diffusion impedance decreases considerably with the temperature increase. Numerical evaluation of the diffusion coefficient of Li in the graphite anode or the LiNiO_2 cathode is impossible as the concentrations of diffusing species in the solid state have been unknown.

4. CONCLUSION

The solvent used to lower flammability - sulfolane, has a high melting point of $27.5 \text{ }^\circ\text{C}$. Sulfolane would greatly limit the range of temperatures where it can be used. For these reason we need to add lithium salts, which modify mixture facilitating better use in li-ion batteries. The study tested the addition of salts (LiPF_6 , LiNTf_2 and LiBOB) to sulfolane and efficiency for each cell cathode.

1. These results show that sulfolane with an addition of LiPF_6 , LiNTf_2 and LiBOB can be a good electrolyte for application in Li-ion batteries using cathode: LiNiO_2 Charging/discharging capacity was stable and occurs between $200\text{-}180 \text{ mAh g}^{-1}$ for $\text{LiNiO}_2|\text{Li}$ system. The value is depend on the current rate. Coulombic efficiency was 90-95 %.

2. Moreover these electrolytes: 1 M LiPF_6 in TMS + 10% VC; 1 M LiNTf_2 in TMS + 10% VC and 1 M LiBOB in TMS+ 10% VC have good cathodic stability and flash points above $160 \text{ }^\circ\text{C}$.

3. It can be seen from the thermal gravimetric analysis (TG/DTA) of the electrolytes under nitrogen atmosphere that the main decomposition peak of the electrolyte (both liquid solvents and the lithium salt) is present at ca. 275 °C.

ACKNOWLEDGEMENTS

Support of grant 03/31/DSPB/0355 is gratefully acknowledged.

References

1. N.A. Kyeremateng, F. Dumur, P. Knauth, B. Pecquenard, T. Djenizian, *Electrochem. Commun.*, 13 (2011) 894.
2. J.F.M. Oudenhoven, L. Baggetto, P.H.L. Notten, *Adv. Energ. Mater.*, 1 (2011) 10.
3. P. Jeevan Kumar, K. Jayanth Babu, O.M. Hussain, *Adv. Sci. Eng. Med.*, 4 (2012) 190.
4. K. Jayanth Babu, P. Jeevan Kumar, O.M. Hussain, C.M. Julien, *J. Solid State Electrochem.*, 16 (2012) 3383.
5. A. Rougier, P. Gravereau, C. Delmas, *J. Electrochem. Soc.*, 143 (1996) 1168.
6. B. Peng, J. Chen, *Coordin. Chem. Rev.*, 253 (2009) 2805.
7. N. Douakha, M. Holzappel, E. Chappel, G. Chouteau, L. Croguennec, A. Ott, B. Ouladdiaf, *J. Solid State Chem.*, 163 (2002) 406.
8. J. Morales, C. Perez-Vicente, J.L. Tirado, *Mater. Res. Bull.*, 25 (1990) 623.
9. J.R. Dahn, V. von Sacken, C.A. Michal, *Solid State Ion.*, 44 (1990) 87.
10. A.T. Hewston, B.L. Chamberland, *J. Phys. Chem. Solid.*, 48 (1987) 97.
11. P. Kalyani, N. Kalaiselvi, *Sci. Techn Adv. Mater.*, 6 (2005) 689.
12. T. Ohzuku, H. Konori, M. Nagayama, K. Sawai, *J. Power Sources*, 68 (1997) 545.
13. Z. Lu, X. Huang, H. Huang, L. Chen, J. Schooman, *Solid State Ion.*, 120 (1999) 103.
14. M. Broussely, F. Pertion, J. Labat, R.J. Staniewicz, A. Romero, *J. Power Sources*, 43-44 (1993) 209.
15. S. Yamada, S.M. Fujiwara, M. Kanda, *J. Power Sources*, 54 (1995) 209.
16. H. Arai, S. Okada, Y. Sakurai, J. Yamaki, *Solid State Ion.*, 109 (1998) 295.
17. Z.F. Ma, X.Y. Yang, X.Z. Liao, X. Sun, J. McBreen, *Electrochem. Commun.*, 3 (2001) 425.
18. K.K. Lee, K.B. Kim, *J. Electrochem. Soc.*, 147 (2000) 1709.
19. Y. Cho, Y.J. Kim, B. Park, *Chem. Mater.* 12 (2003) 3788.
20. Y. Cho, G.B. Kim, H.S. Lim, C.S. Kim, S.Y. Yoo, *Electrochem. Solid-State Lett.*, 2 (1999) 607.
21. Y. Cho, G.B. Kim, H.S. Lim, C.S. Kim, S.Y. Yoo, *Electrochem. Solid-State Lett.*, 4 (2001) 159.
22. Y.S. Lee, Y.K. Sun, K.S. Nahm, *Solid State Ion.*, 118 (1999) 159.
23. H. Liu, Z. Zhang, Z. Gong, Y. Yang, *Electrochim. Acta*, 49 (2004) 1151.
24. A. Lewandowski, B. Kurc, I. Stepniak, A. Swiderska-Mocek, *Electrochim. Acta*, 56 (2011) 5972.
25. 25 Martinmaa J, Lagowski JJ (1976) Sulfolane in The Chemistry of Nonaqueous Solvents. Academic Press, New York
26. V.S. Kolosnitsyn, L.V. Sheina, S.E. Mochalov *Russ J. Electrochem.*, 44 (2008) 575.
27. J. Hassoun, P. Reale, S. Panero, B. Scrosati, M. Wachtler, M. Fleischhammer, M. Kasper, M. Wohlfahrt-Mehrens *Electrochim. Acta*, 55 (2010) 145.
28. C. H. Lu and L. Wei-Cheng, *J. Mater. Chem.*, 10 (2000) 1403.
29. K.S. Park, S.H. Park, Y.K. Sun, K.S. Nahm, Y.S. Lee, M. Yoshio, *J. Appl. Electrochem.*, 32 (2002) 1229.
30. H. Arai, S. Okada, H. Ohtsuka, M. Ichimura and J. Yamaki, *Solid State Ion.*, 80 (1995) 261.
31. J. Xu, L. Feng, D. Nordlund, Ethan J. Crumlin, F. Wang, J. Bai, M.M. Doeff, T. Wei *Chem. Commun.*, 52 (2016) 4239.

32. X. Zheng, Xiaobo X. Li, X. Wang, Zng. Guo, Huajun *Electrochim. Acta*, 191 (2016) 832.
33. S. Xu Ch. Du, X. Xu, G. Han, P. Zuo, X. Cheng, Y. Ma, G. Yin *Electrochim. Acta*, 248 (2017) 534.
34. K. Yo, T. Mitsuharu, M. Hajime, K. Nobuhiro, *J. Power Sources*, 364 (2017) 156.
35. H.K. Shin, J. H. Kim, J. Wang, J. Dae Leea, *J. Power Sources*, 372 (2017) 107.
36. X. Jin, W. Feng, Ch. Renji, L. Li, Y. Huigen *J. Power Sources*, 233 (2013) 115.
37. A. Lewandowski, B. Kurc, A. Swiderska-Mocek, N. Kusa, *J. Power Sources*, 266 (2014) 132.

© 2018 The Authors. Published by ESG (www.electrochemsci.org). This article is an open access article distributed under the terms and conditions of the Creative Commons Attribution license (<http://creativecommons.org/licenses/by/4.0/>).